

Magnetic Behavior of $\text{La}_7\text{Ru}_3\text{O}_{18}$

P. Khalifah

Department of Chemistry and Princeton Materials Institute, Princeton University, Princeton, New Jersey 08540

D. A. Huse

Department of Physics, Princeton University, Princeton, New Jersey 08540

R. J. Cava

Department of Chemistry and Princeton Materials Institute, Princeton University, Princeton, New Jersey 08540

(November 15, 2018)

Rhombohedral $\text{La}_7\text{Ru}_3\text{O}_{18}$ can be considered to be nearly geometrically frustrated due to its close structural similarity to the strongly geometrically frustrated compound $\text{La}_{4.87}\text{Ru}_2\text{O}_{12}$. The magnetic ordering of $\text{La}_7\text{Ru}_3\text{O}_{18}$ was explored using a combination of dc and ac magnetic susceptibility measurements. The magnetic phase diagram shows two different ordering regimes. A low field magnetic phase occurs at applied fields of 0-3T and temperatures below 10K, while a high field phase is found at fields of 3-5T and temperatures below 9K.

I. INTRODUCTION

The long range ordering of a compound with antiferromagnetic interactions between spins can be hindered by certain geometric arrangements of the magnetic ions [1]. This phenomena of geometric frustration is known to occur for a number of different structures with magnetic ions patterned in specific highly symmetric arrangements in two or three dimensions. For two-dimensional structure types, both triangular and kagomé lattices of magnetic atoms can lead to geometric frustration. Good examples of frustration due to triangular lattices can be found in delafossite-type compounds such as LiCrO_2 [2] and NaTiO_2 [3], while frustration has been extensively studied in kagomé lattice compounds such as $\text{SrCr}_8\text{Ga}_4\text{O}_{12}$ [4] which crystallize in the magnetoplumbite structure. Although a greater degree of lattice complexity has been observed for three-dimensional geometrically frustrated antiferromagnets, the basic building blocks of these 3D lattices are triangles and tetrahedra. Some compounds that are frustrated because of their three-dimensional lattice are the garnet $\text{Gd}_3\text{Ga}_5\text{O}_{12}$ [5], the spinel ZnCr_2O_4 [6], the FCC compound K_2IrCl_6 [7], and the pyrochlore $\text{Dy}_2\text{Ti}_2\text{O}_7$ [8].

$\text{La}_7\text{Ru}_3\text{O}_{18}$ has a rhombohedral structure closely related to that of monoclinic $\text{La}_{4.87}\text{Ru}_2\text{O}_{12}$, a compound previously reported to be a strongly geometrically frustrated antiferromagnet [9]. Despite the structural similarities, $\text{La}_7\text{Ru}_3\text{O}_{18}$ is at most only moderately frustrated, with a frustration index of $f = -\theta/T_N \cong 6$. Ru atoms in the ab plane of both compounds are patterned in a triangular lattice. Each in-plane triangle of Ru atoms is capped by a fourth Ru atom in a neighboring plane, giving rise to a tetrahedral arrangement of Ru atoms in three dimensions, as illustrated in fig. 1. There are three distinct Ru sites in the crystal structure. $\text{La}_7\text{Ru}_3\text{O}_{18}$ was previously found to have a moment of $3.49 \mu_B$, and a Curie-Weiss constant of -58K which indicates medium strength antiferromagnetic interactions between spins [9]. In the course of that initial investigation of $\text{La}_7\text{Ru}_3\text{O}_{18}$, behavior more complex than that expected for a simple antiferromagnet was observed. Here we report a more detailed study of the magnetic behavior of $\text{La}_7\text{Ru}_3\text{O}_{18}$,

and show that it has an unusual magnetic phase diagram at low temperatures.

II. EXPERIMENTAL

Starting materials were dried La_2O_3 (99.99%, Alfa) and RuO_2 (99.9%, Cerac). $\text{La}_7\text{Ru}_3\text{O}_{18}$ was made by mixing La_2O_3 and RuO_2 in the stoichiometric ratio or with a slight Ru excess. The powders were placed in dense alumina crucibles and heated at 775, 850, and 875 °C for at least two days each with multiple intermediate grindings. Samples were then annealed for about two weeks at 875 °C with multiple regrindings until judged to be single phase by powder x-ray diffraction.

Both ac and dc magnetic susceptibility measurements were performed on the Physical Property Measurement System (PPMS, Quantum design). Field cooled (FC) measurements were done by applying the field, cooling the sample, and then measuring the temperature dependence of the magnetic susceptibility upon heating. Field sweeps were done by ramping the field from 9T to -9T to 9T. The ac susceptibility measurements were done at a frequency of 10kHz with an amplitude of 12Oe. All ac susceptibility measurements made in the presence of a constant dc field were done with field cooling.

III. RESULTS AND DISCUSSION

$\text{La}_7\text{Ru}_3\text{O}_{18}$ obeys the Curie-Weiss behavior at temperatures above 60K for all applied fields studied (0-9T), as seen in the inset to fig. 2. There is no difference between the field cooled and zero-field cooled data (not shown), indicating that the low temperature drop in the magnetic susceptibility (fig. 2, main panel) represents a transition to a long range ordered antiferromagnetic ground state rather than a spin glass ground state. Although the manner in which the field was applied does not affect the data, the magnitude of the field does. The maximum in the absolute susceptibility ($\chi_{dc} = M/H$) is at 14K at an applied field of 1T, and drops to 9K as the applied field is increased to 9T. Furthermore, the magnitude of the low temperature dc susceptibility ($\chi_{dc} = M/H$) increases with increasing applied field in the range of $0 < H < 7\text{T}$. For antiferromagnets, increasing the applied field has no effect on χ_{dc} until sufficiently high fields are reached, leading to saturation of the spins and causing χ_{dc} to decrease with further increases in H . Since there is no simple explanation for the field behavior of χ_{dc} , it seems that $\text{La}_7\text{Ru}_3\text{O}_{18}$ may have multiple types of magnetic ordering.

In order to better understand the atypical field behavior of the low temperature susceptibility, field sweep measurements were made at a variety of temperatures. Below 15K, two distinct features were present in these M vs. H loops, and at 5K and below, hysteresis was observed. M vs. H data collected at 2.5K is shown in fig. 3, with hysteresis clearly visible in both the low field ($\sim 3\text{T}$) and high field ($\sim 5\text{T}$) regimes. It is therefore apparent that two distinct magnetic phase transitions can be induced in $\text{La}_7\text{Ru}_3\text{O}_{18}$ by applying a magnetic field.

The two features in the M vs. H data can be more clearly resolved by plotting the differential susceptibility, dM/dH , shown in fig. 4. The two maxima in the derivative plots mark the location of the low field and high field magnetic phase transitions. The positive and negative field portions of the plots very accurately mirror each other, confirming the quality of the data. The close proximity of the low field and high field transitions at 7.5K make it impossible to precisely locate the center of the low field transition. In the lowest temperatures (2.5 and 5K), the location of both transitions depends on the measurement history. At these temperatures, there is an upper and a lower phase boundary for both the high field and the low field transition due to the observed hysteresis.

A second, complimentary means of observing the magnetic phase boundaries is measurement of the ac susceptibility, χ_{ac} . Measurements of χ_{ac} can scan temperature while keeping the applied field fixed, while M vs H scans fix the temperature and vary the field. Unlike the dM/dH plots, the χ_{ac} data can accurately map the phase boundaries near the zero-field transition temperature. The results of the ac susceptibility measurements on $\text{La}_7\text{Ru}_3\text{O}_{18}$ are shown in fig. 5.

Peaks are observed in two temperature ranges in the χ_{ac} scans. Figure 5 shows the higher temperature peak. It can be seen that the shape of this peak changes from broad and asymmetric to sharp and more symmetric as the field is increased from 0T to 5T. Above 5T the intensity of the peak rapidly decreases. It can be seen that a low-temperature peak is present for the 3T data. A low temperature peak is found only within a narrow window ($\sim 0.25\text{T}$) of applied fields near 3T (data not shown). The location of the peak shifts to lower temperatures with increasing field. The very low temperature of this second ac transition ($< 4\text{K}$) prevented a detailed determination of the low temperature phase boundary, although one data point could be plotted in the overall magnetic phase diagram.

Combining the dM/dH and the χ_{ac} data allows the magnetic phase diagram of $\text{La}_7\text{Ru}_3\text{O}_{18}$ to be drawn (fig. 6). Two definite magnetic phases are labelled in the diagram. The dM/dH data clearly define the horizontal field boundaries between the different phases, while the ac susceptibility data provide the best measure of the transition temperatures of the phases. We note that for ac susceptibility measurements with applied fields of $\leq 2\text{T}$, the transition temperature was taken to be the point of maximum slope in χ_{ac} vs. T rather than the peak maximum due to the broad shape of the peak at low fields. Even though the highest field ($H \geq 6\text{T}$) measurements of χ_{ac} still show a peak maximum, these points were not plotted on the phase diagram due to the broader and weaker character of the peaks. Similarly, the peaks observed in dM/dH plots for $T \geq 10\text{K}$ were no longer sharp and were not plotted in the phase diagram. The observation of weak features outside the plotted limits of the magnetic phase diagram reflects the difficulty of defining sharp boundaries for magnetic phase transition, which often involve continuous and gradual spin rearrangements in addition to exhibiting short range correlations at temperatures just above the onset of long-range order.

IV. CONCLUSIONS

Since the both the low field (3T) and high field transition (5T) involve a jump in the magnetization due to the increasing magnetic field, these transitions should involve spin reorientation, with spins moving from an axis defined by the crystal fields or the antiferromagnetic interactions to an axis defined by the magnetic field. From previously published structural data [9], it is known that there are two different types of layers in $\text{La}_7\text{Ru}_3\text{O}_{18}$. The thicker layer has a 2.67:1 La:Ru ratio while the thinner layer has a 2:1 La:Ru ratio and has two inequivalent Ru sites. The different crystal environments may give rise to crystals fields of different strengths on the different Ru spins, with the effect that different magnetic field strengths are necessary to dislodge the spins from the crystal field in each type of Ru site. It should be noted that since $\mu g H/k$ is 18 K for an applied field of 9T, the energy scale of the applied field exceeds that of the antiferromagnetic ordering ($T_N \sim 10$ K), where μ is the moment of $S = 3/2$ Ru, The g -factor $\cong 2$, H is the applied field, and k is the Boltzmann constant. Even though our data is from a powder sample, it is unlikely that the two transitions represent two different orientations of the grains in our powder since no evidence of preferred orientation was observed in previous structural studies [9]. Although it is interesting to speculate on the nature of the different magnetic phases, it is difficult to make definite conclusions about the precise nature of the magnetic ordering in the absence of neutron diffraction data or single crystal magnetization measurements.

V. ACKNOWLEDGEMENT

This research was supported by the NSF Solid State Chemistry and Polymers program, grant No. DMR-9725979. Thanks go to B. Sales for insightful comments on the manuscript.

-
- [1] A. P. Ramirez, Ann. Rev. Mater. Sci. **24**, 453 (1994).
 - [2] A. Tauber, W. M. Moller, and E. Banks, J. Solid State Chem. **4**, 138 (1972).
 - [3] K. Hirakawa, H. Kadowaki, and K. Ubukoshi, J. Phys. Soc. Jpn. **54**, 3526 (1985).
 - [4] P. Schiffer, A. P. Ramirez, K. N. Franklin, and S. W. Cheong, Phys. Rev. Lett. **77**, 2085 (1996).
 - [5] S. Hov, H. Bratsberg, and A. T. Skjeltorp, J. Magn. Magn. Mater. **15-18**, 455 (1980).
 - [6] P. K. Baltzer, P. J. Wojtowicz, M. Robbins, and E. Lopatin, Phys. Rev. **151**, 367 (1966).
 - [7] A. H. Cooke, R. Lazenby, F. R. McKim, J. Owen, and W. P. Wolf., Proc. R. Soc. London Ser. A. **250**, 97 (1959).
 - [8] A. P. Ramirez, C. L. Broholm, R. J. Cava, and G. R. Kowach, Physica B **280**, 290 (2000).
 - [9] P. Khalifah, Q. Huang, D. M. Ho, H. W. Zandbergen, and R. J. Cava, J. Solid State Chem. **155**, 189 (2000).

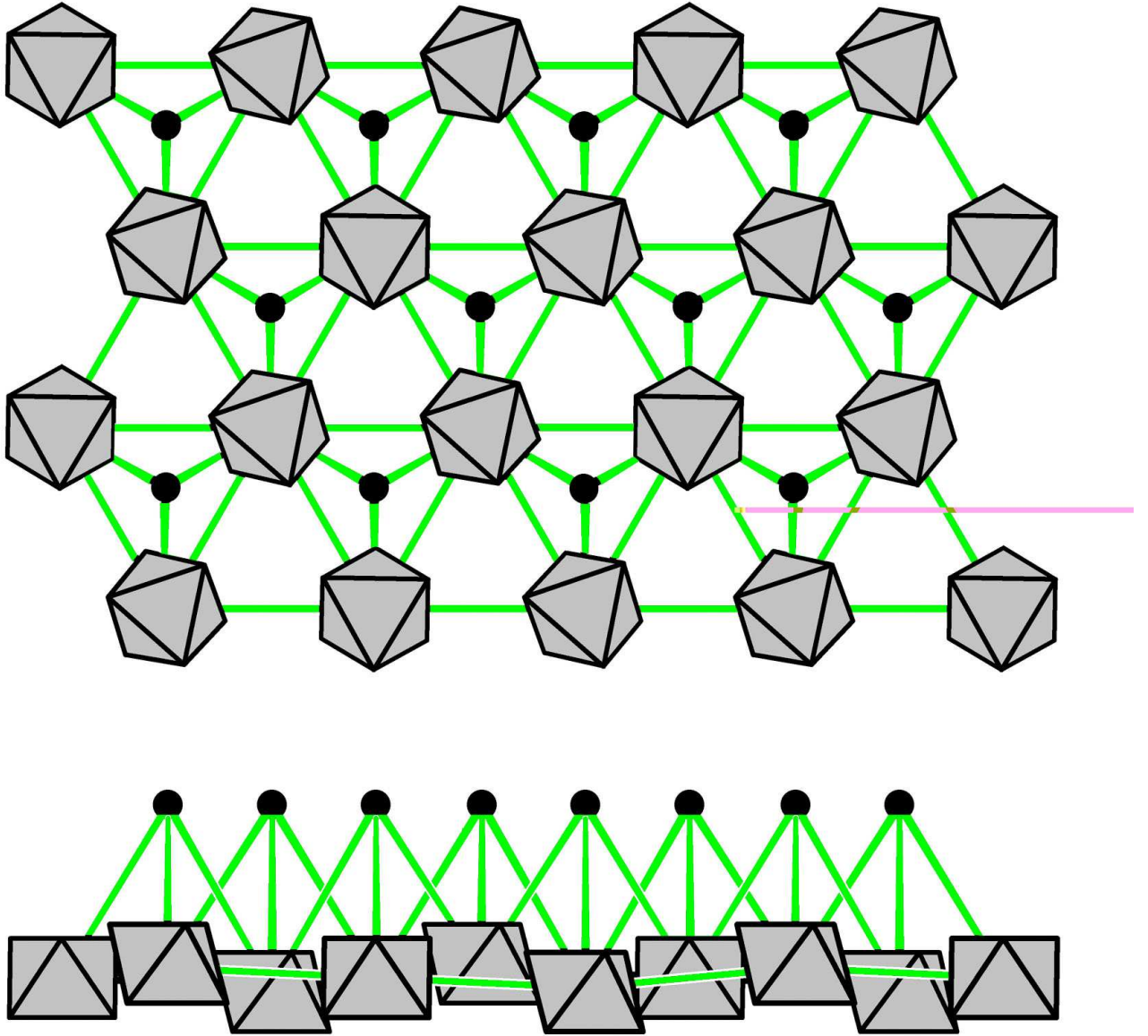


FIG. 1. Top: View perpendicular to a plane of RuO_6 octahedra (gray) showing the triangular arrangement of Ru atoms in two dimensions. Ru atoms are at the center of the RuO_6 octahedra while O atoms are at the vertices. Ru atoms in the next higher plane (shown in black) cap the RuO_6 octahedra, giving rise to a tetrahedral arrangement of Ru sites in three dimensions. Bottom: in-plane view, highlighting the tetrahedral arrangement.

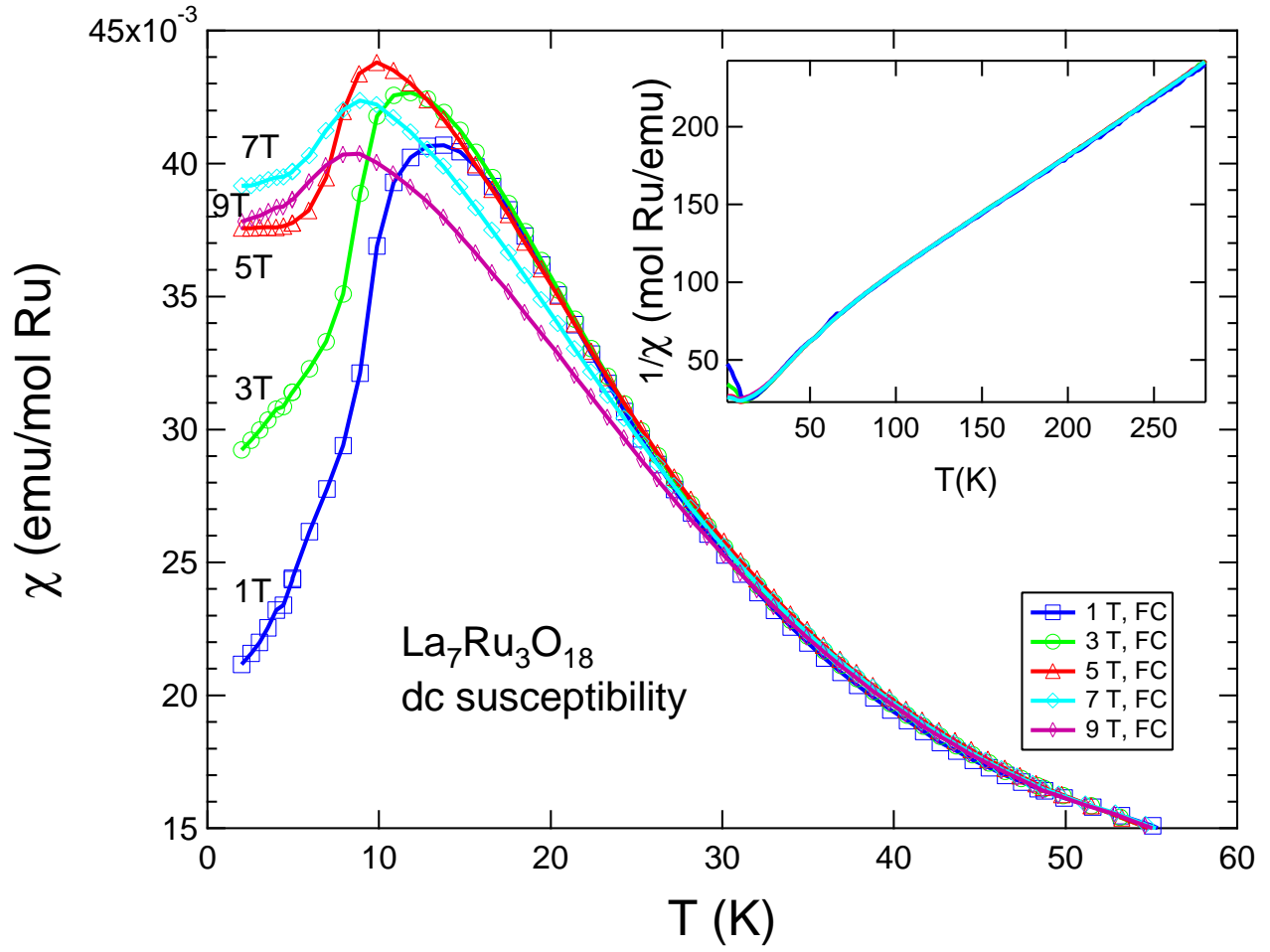


FIG. 2. Magnetic susceptibility ($\chi_{dc} = M/H$) at low temperatures. Inset shows linearity and field-independence of $1/\chi_{dc}$ at higher temperatures. Data for $H=1\text{T}$, 3T , 5T , 7T , and 9T are superimposed.

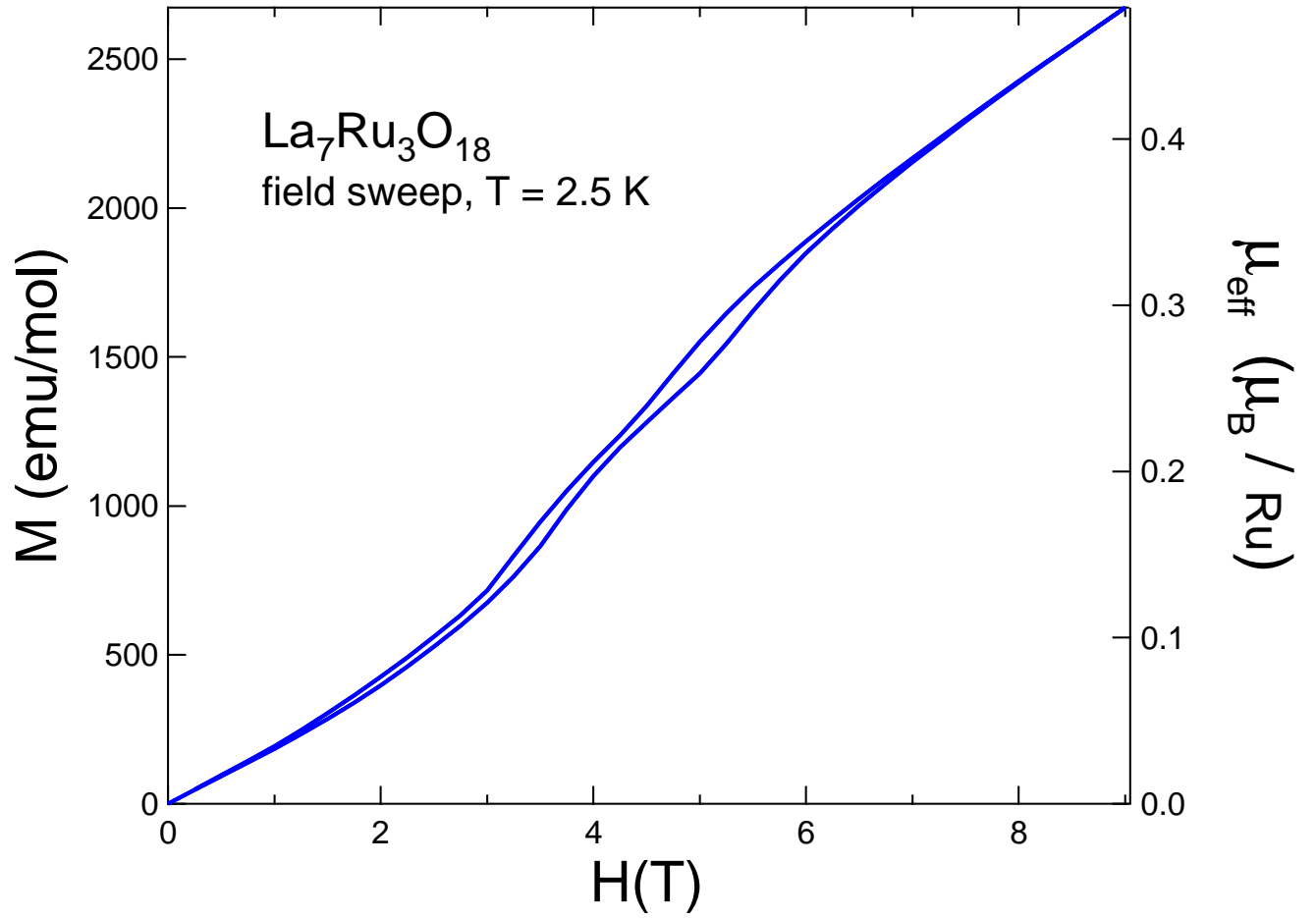


FIG. 3. Field dependence of magnetization at $T = 2.5\text{K}$ showing the two distinct regions of hysteresis. Only the data for $H > 0$ are shown.

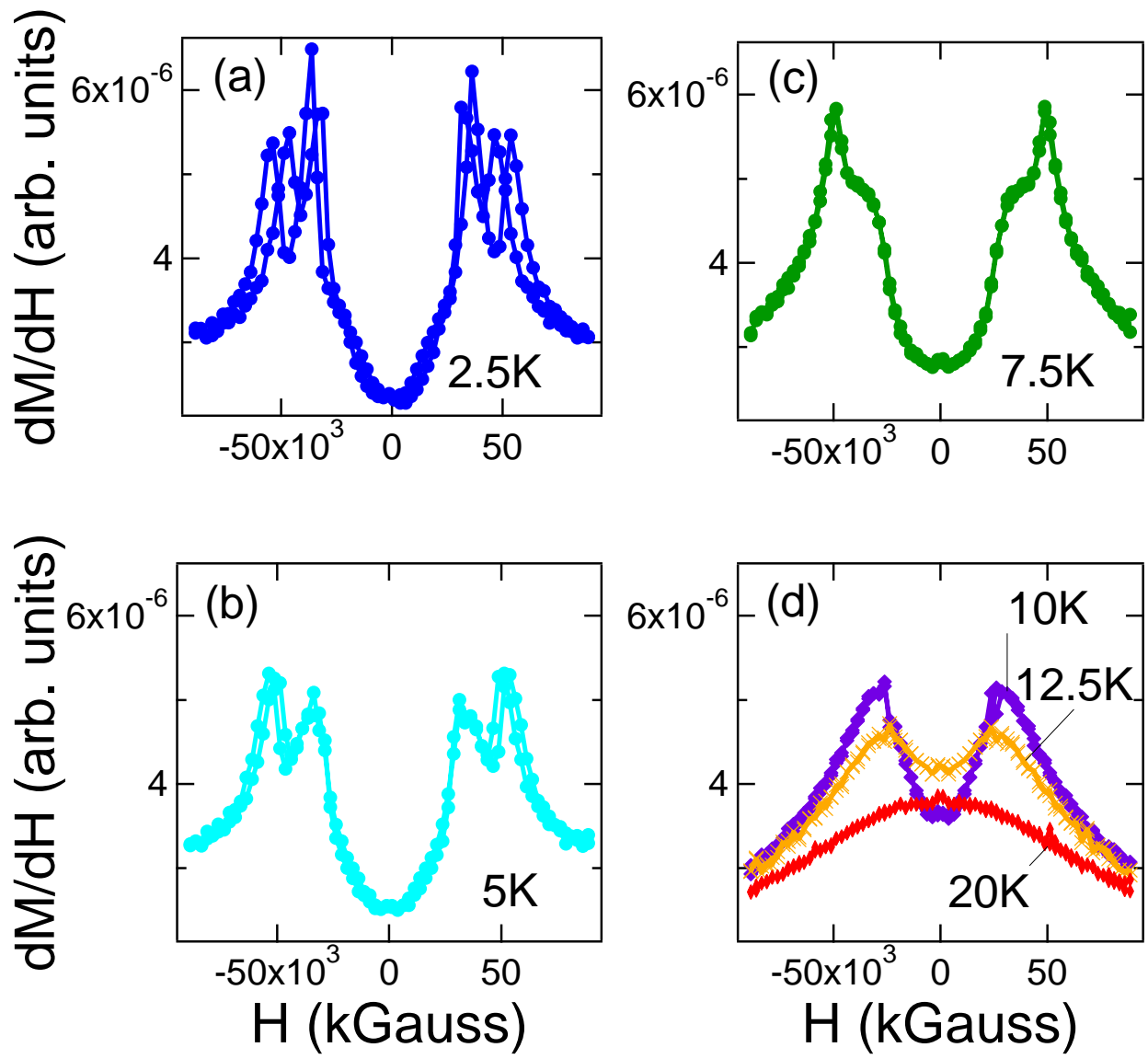


FIG. 4. Field dependence of dM/dH at (a) 2.5K, (b) 5K, (c) 7.5K, (d) 10, 12.5, and 20 K.

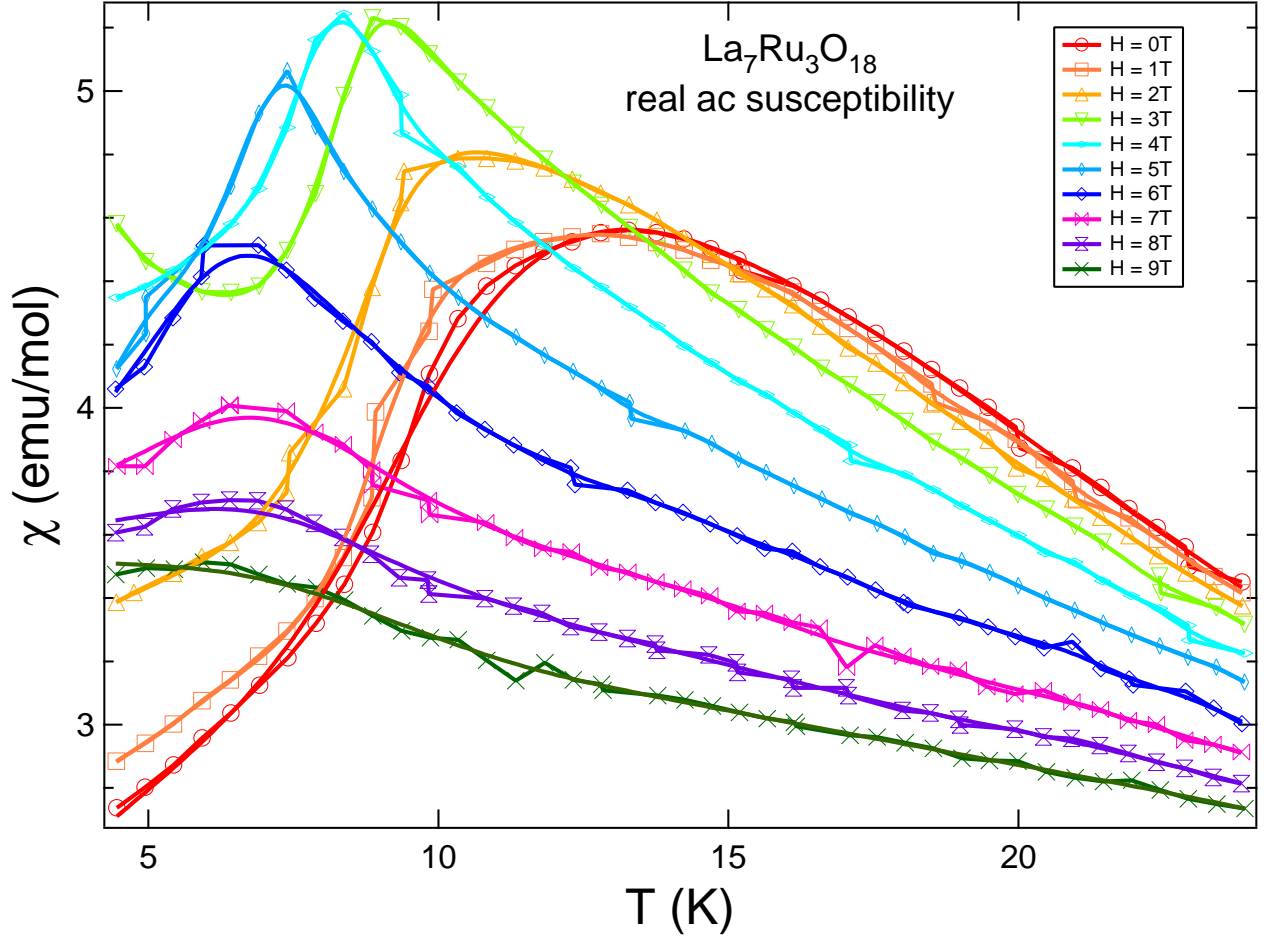


FIG. 5. The real portion of the ac susceptibility (χ'_{ac}) of $\text{La}_7\text{Ru}_3\text{O}_{18}$. Solid lines are a guide to the eye.

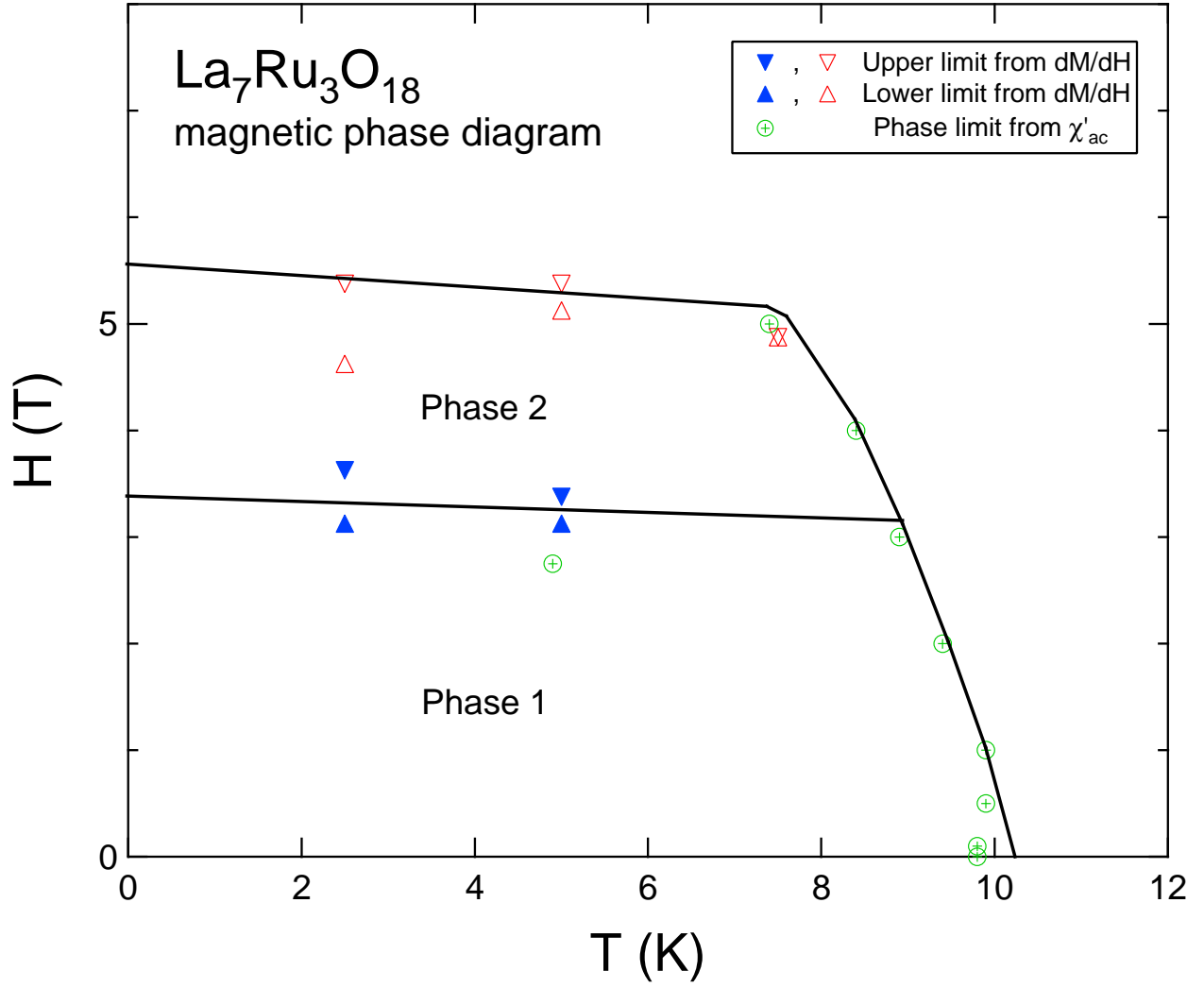


FIG. 6. Magnetic phase diagram of La₇Ru₃O₁₈. Solid lines are a guide to the eye.